EPJ Web of Conferences **303**, 01004 (2024) https://doi.org/10.1051/epjconf/202430301004
MENU 2023

The $\Lambda(1405)$ pole structure from Lattice QCD: a coupled-channel $\pi\Sigma - \bar{K}N$ study

John Bulava[1,], *Bárbara* Cid-Mora[2,3,*], *Andrew D.* Hanlon[4,], *Ben* Hörz[5,], *Daniel* Mohler[3,2,], *Colin* Morningstar[6,], *Joseph* Moscoso[7,], *Amy* Nicholson[7,], *Fernando* Romero-López[8,], *Sarah* Skinner[7,], and *André* Walker-Loud[9,]

[1]Fakultät für Physik und Astronomie, Institut für Theoretische Physik II, Ruhr-Universität Bochum, 44780 Bochum, Germany
[2]GSI Helmholtz Centre for Heavy Ion Research, Darmstadt, Germany
[3]Institut für Kernphysik, Technische Universität Darmstadt, Schlossgartenstrasse 2, 64289 Darmstadt, Germany
[4]Physics Department, Brookhaven National Laboratory, Upton, New York 11973, USA
[5]Intel Deutschland GmbH, Dornacher Str. 1, 85622 Feldkirchen, Germany
[6]Department of Physics, Carnegie Mellon University, Pittsburgh, Pennsylvania 15213, USA
[7]Department of Physics and Astronomy, University of North Carolina, Chapel Hill, NC 27516-3255, USA
[8]Center for Theoretical Physics, Massachusetts Institute of Technology, Cambridge, MA 02139, USA
[9]Nuclear Science Division, Lawrence Berkeley National Laboratory, Berkeley, CA 94720, USA

Abstract.
This report summarizes results of the first lattice QCD calculation of coupled-channel $\pi\Sigma - \bar{K}N$ scattering in the $\Lambda(1405)$ region. This study was carried out using a single CLS ensemble with a heavier-than-physical pion mass $m_\pi \approx 200$ MeV and a lighter-than-physical kaon mass $m_K \approx 487$ MeV. Once the finite-volume energy spectrum has been reliably extracted, the Lüscher method was employed to obtain scattering amplitudes. Through a variety of parametrizations of the two-channel K-matrix, the final results show a virtual bound state below the $\pi\Sigma$ threshold and a resonance right below $\bar{K}N$.

1 Introduction

The $\Lambda(1405)$ baryon is considered a puzzling state when trying to accommodate it within conventional quark models, and several studies have been conducted in order to tackle and understand it (see Refs. [1, 2] for a more extensive review). This 4-star state (according to [3]) with $I(J^P) = 0(\frac{1}{2}^-)$ and strangeness $S = -1$ was initially predicted in [4]. In their work, the analysis of low-energy $K^- p$ scattering amplitudes implied a resonance in the 1405 MeV region. This was later experimentally confirmed in [5] when looking into the $\pi\Sigma$ mass spectrum. From the variety of approaches investigating the $\Lambda(1405)$, important aspects to address this state have emerged, such as the importance of including meson-baryon components in the scattering analysis [6, 7], and the concept of a two-pole picture in the complex energy plane of the scattering amplitude [8]. The latter was further explored in [9, 10], suggesting

*e-mail: b.cidmora@gsi.de

that resonances like the $\Lambda(1405)$ can be dynamically generated by underlying meson-baryon interactions, which result in two poles in this energy region. Moreover, while there are many lattice QCD studies that have been done to learn about this baryon, none of them extracted the full spectrum including the $\pi\Sigma - \bar{K}N$ coupled-channel scattering analysis.

This first lattice QCD calculation determining the $\pi\Sigma - \bar{K}N$ coupled-channel scattering amplitude [11, 12] was carried out using a single ensemble and included not only single-hadron operators, but also meson-baryon interpolating fields. This study aims to address the long-standing disagreement regarding whether there is one or two poles and their positions in the complex energy plane. In order to do so, the Lüscher method [13, 14] is utilized, since it has been shown to be a powerful tool to access the hadron scattering amplitudes and infer resonance properties. This method connects the continuum scattering amplitudes to the finite-volume energy spectra obtained from lattice QCD calculations [15].

This report is organized such that Section 2 briefly summarizes all details of the lattice techniques utilized to carry out the study, including the tools used to compute correlation function matrices and the methodologies used to diagonalize and fit them, as well as final results of the finite-volume energy spectra. Later, Section 3 introduces the Lüscher formalism and the main results of the coupled-channel $\pi\Sigma - \bar{K}N$ scattering amplitude analysis and the position of the poles when analytically continued to the complex energy plane. Finally, Section 4 summarizes the main results, the importance of the methods used, and future paths.

2 Lattice details and correlation functions

This section introduces the most important details of the ensemble of QCD gauge configurations used in this study [11, 12]. The finite-volume energy spectra extracted were computed and are shown in Figure 3.

Lattice details. – A single ensemble of QCD gauge configurations generated by the Coordinated Lattice Simulations consortium (CLS) was employed: namely D200 [16]. These gauge field configurations have heavier-than-physical degenerate u- and d-quarks and a lighter-than-physical s-quark. These were generated with the tree-level improved Lüscher-Weisz gauge action, and a non-perturbatively $O(a)$-improved Wilson fermion action. Also, open temporal boundary conditions were used in order to reduce autocorrelation of the global topological charge. Additional information about the gauge field configurations is summarized in Table 1.

Correlators. – Euclidean time correlation functions were computed using the stochastic Laplacian Heaviside method (sLapH) [17, 18], these included single- and multi-hadron operators with different momentum combinations: $\Lambda(\vec{\mathbf{P}})$, $\pi(\vec{\mathbf{P}}_1)\Sigma(\vec{\mathbf{P}}_2)$ and $\bar{K}(\vec{\mathbf{P}}_1)N(\vec{\mathbf{P}}_2)$. These correlation functions satisfy

$$C_{ij}(t) = \langle \mathcal{O}_i(t)\bar{\mathcal{O}}_j(0)\rangle = \sum_n A_n \mathrm{e}^{-tE_n}. \tag{1}$$

Where the multi-hadron correlators in Eq. (1) needed to be diagonalized to obtain the finite-volume energy levels. This diagonalization was achieved by solving the Generalized Eigenvalue Problem (GEVP) [19, 20].

a[fm]	$(L/a)^3 \times T/a$	am_π	am_K	$m_\pi L$
0.0633(4)(6)	$64^3 \times 128$	0.06533(25)	0.15602(16)	4.181(16)

Table 1. Properties of the CLS D200 ensemble. a is the lattice spacing and $L^3 \times T$ is the lattice extent.

Finite-volume energy spectra. – Once the correlation matrices were built and diagonalized, the fitting and analysis phase begins. In this step, the diagonalized correlators were fitted employing correlated-χ^2 fits over different time intervals (labelled $[t_{\text{min}}, t_{\text{max}}]$), and based on a variety of fit forms. These include single exponential, two-exponential, and geometric series ansatzes (see Figure 1 for example results of the pion). The multi-hadron correlators also incorporated a ratio of correlator fits (see Figure 2 for an example of fit forms of the multi-hadron correlators). The final finite-volume energy spectra extracted are shown in Figure 3, and only levels below the three particle threshold ($\pi\pi\Lambda$) are taken into account for the scattering amplitude analysis.

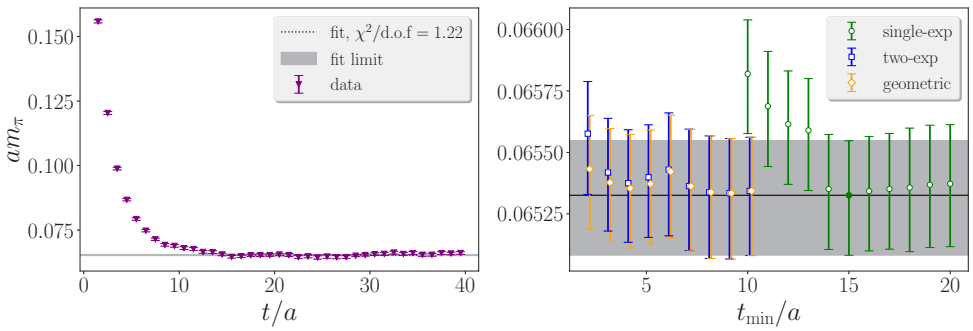

Figure 1. (Left) Effective energy of the pion mass in purple, and corresponding fit in gray. (Right) Different fit form results for the pion correlator versus t_{min}. The correlated-χ^2s were computed over the range $[t_{\text{min}}, t_{\text{max}}]$, where the chosen t_{min} is expected to reduce excited states contamination. The final results were chosen so that there is consistency among the fit forms.

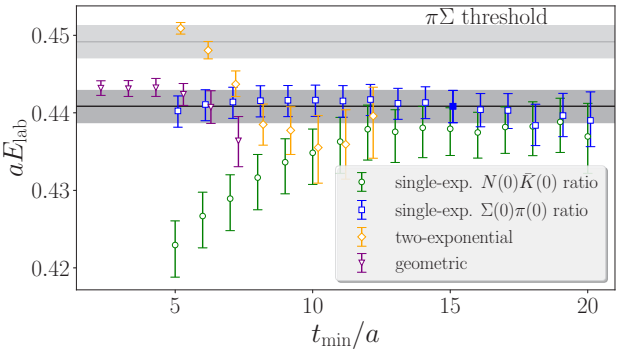

Figure 2. Example results of the G_{1u} irrep for a variety of fit forms versus t_{min}. The ratio of correlators was done using a single exponential ansatz to a ratio of the diagonal correlator over the nearby non-interacting $\bar{K}(\vec{\mathbf{P}}_1)N(\vec{\mathbf{P}}_2)$ or $\pi(\vec{\mathbf{P}}_1)\Sigma(\vec{\mathbf{P}}_2)$ level (see Refs. [11, 12] for more details).

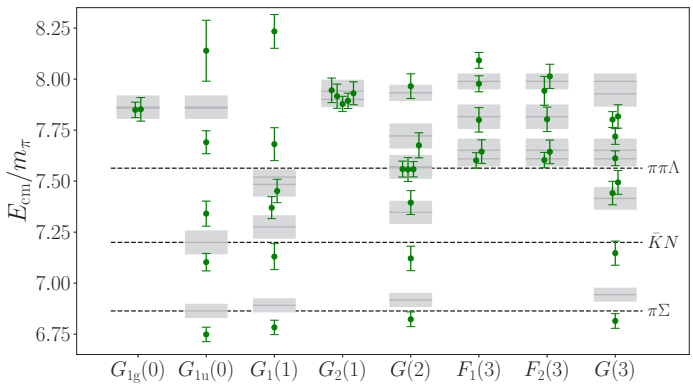

Figure 3. Final finite-volume energy spectra used as a constraint in the scattering amplitude analysis. In this plot, dashed lines correspond to scattering thresholds, gray lines and bands are the non-interacting levels (sum of energies of non-interacting hadrons) with increasing momenta, and green points are the finite-volume energy spectrum in the center-of-mass frame with their bootstrap error.

3 Scattering amplitudes

This section introduces the Lüscher formalism the associated quantization condition that relates the finite-volume stationary-state energy spectra with the continuum scattering amplitudes, and the final results of the positions of the poles.

Lüscher formalism. – This method is a useful tool to extract information about resonances. This connection arises from the following condition

$$\det\left[\widetilde{K} + F^{-1}\right] = 0, \tag{2}$$

where $\widetilde{K}$ is the parametrized scattering matrix and F^{-1} is the "box matrix" for a particular total momentum $\mathbf{P} = (2\pi/L)\mathbf{d}$ (with $\mathbf{d} \in \mathbb{Z}^3$) and it encodes information of the lattice and the breaking of rotational symmetry. The importance of this determinant condition lies on the relation the $\widetilde{K}$-matrix has with the scattering transition amplitude. This is used to relate lattice results with the position of the poles in the complex energy plane of the scattering transition amplitude when analytically continued.

K−matrix parametrization. – Once the finite-volume energy spectra are extracted, the quantization condition in Eq. (2) takes the following form for the coupled-channel $\bar{K}N - \pi\Sigma$:

$$\det\left[\begin{pmatrix} \widetilde{K}_{\pi\Sigma\to\pi\Sigma} & \widetilde{K}_{\pi\Sigma\to\bar{K}N} \\ \widetilde{K}_{\bar{K}N\to\pi\Sigma} & \widetilde{K}_{\bar{K}N\to\bar{K}N} \end{pmatrix} + \begin{pmatrix} F^{-1}_{\pi\Sigma}(E_n, \vec{P}, L) & 0 \\ 0 & F^{-1}_{\bar{K}N}(E_n, \vec{P}, L) \end{pmatrix}\right] = 0. \tag{3}$$

In this description, the multi-channel $\widetilde{K}$-matrix was parametrized and constrained by the finite-volume energy spectra extracted from lattice. A thorough list of parametrizations were employed to study the behavior of the pole positions in the complex energy plane. Below is the Effective Range Expansion (ERE) parametrization as an example (see [11, 12] for the full list)

$$\frac{E_{\rm cm}}{m_\pi}\widetilde{K}_{ij} = A_{ij} + B_{ij}\Delta_{\pi\Sigma}, \tag{4}$$

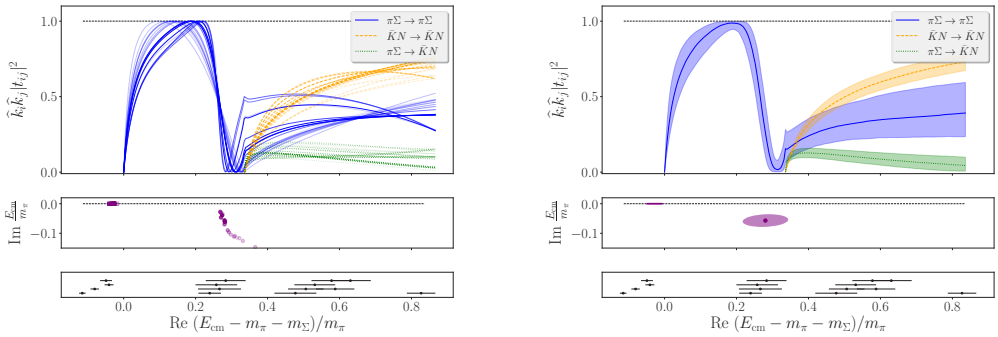

Figure 4. Scattering transition amplitude results as a function of energy in the center-of-mass frame over the pion mass. t_{ij} and k_{ij} are defined in Eq. (6), and i, j are the flavor channels. (Left) The upper panel shows the transition amplitudes for several parametrizations. The transparency parameter is associated to AIC results, where darker lines correspond to a lower AIC. The middle panel depicts the position of the poles in the complex energy plane, and the bottom panel contains the finite-volume energy spectra used to constrain the fits. (Right) Results of the parametrization of the scattering amplitude that had the best fit, where uncertainties were estimated by bootstrap resampling.

where

$$\Delta_{\pi\Sigma} = \frac{E_{\rm cm}^2 - (m_\pi + m_\Sigma)^2}{(m_\pi + m_\Sigma)^2}. \tag{5}$$

As shown in Figure 4, various fits were carried out for all the K-matrix parametrizations to check consistency and sensitivity of the results (full set of results in Tables VII to XI of Appendix C in Ref. [11]). The best-fit values were chosen based on the lowest Akaike Information Criterion (AIC). Then the scattering transition amplitude was defined as

$$t^{-1} = \widetilde{K}^{-1} - i\hat{k}, \tag{6}$$

where $\hat{k} = \mathrm{diag}\,(k_{\pi\Sigma}, k_{\bar{K}N})$. Lattice data constrained the coupled-channel $\pi\Sigma - \bar{K}N$ scattering amplitude, hence providing information in this energy range, and enabling the analytical continuation to the complex $E_{\rm cm}$. Eq. (7) can be further written as

$$t = \frac{m_\pi}{E_{\rm cm} - E_{\rm pole}} \begin{pmatrix} c_{\pi\Sigma}^2 & c_{\pi\Sigma}c_{\bar{K}N} \\ c_{\pi\Sigma}c_{\bar{K}N} & c_{\bar{K}N}^2 \end{pmatrix}, \tag{7}$$

where the complex residues $c_{\pi\Sigma}$, $c_{\bar{K}N}$ are the couplings of the resonance poles to each channel. The final results in Figure 4 exhibit two poles in the following positions

$$E_1 = 1392(9)_{\rm st}(2)_{\rm md}(16)_a\ \text{MeV}, \tag{8}$$

$$E_2 = [1455(13)_{\rm st}(2)_{\rm md}(17)_a - i11.5(4.4)_{\rm st}(4)_{\rm md}(0.1)_a]\ \text{MeV}, \tag{9}$$

and the ratios of residues

$$\left|\frac{c_{\pi\Sigma}^{(1)}}{c_{\pi\Sigma}^{(1)}}\right| = 1.9(4)_{\rm st}(6)_{\rm md}, \quad \left|\frac{c_{\pi\Sigma}^{(2)}}{c_{\pi\Sigma}^{(2)}}\right| = 0.53(9)_{\rm st}(10)_{\rm md}. \tag{10}$$

The uncertainties *st*, *md*, *a* correspond to statistical error, model parametrization, and propagated errors from the precision of the lattice scale-setting, respectively. The pole at E_1 couples more strongly to the $\pi\Sigma$ channel and we conclude it corresponds to a virtual bound state,

whereas the pole at E_2 has a stronger coupling to $\bar{K}N$ and is consistence with a resonance. It is noteworthy to mention that, all the K-matrix parametrizations used found two poles in the $\Lambda(1405)$ region, even though they made no assumptions about the number of poles.

4 Conclusion

Lattice QCD is a powerful tool in hadronic physics, since it allows for predictions once the quark masses and the coupling are fixed, and is ab-initio and systematically improvable. In the $\Lambda(1405)$ sector, its use facilitates the exploration of the $\pi\Sigma$ scattering amplitude below the $\bar{K}N$ threshold, where the resulting finite-volume energy spectra is related to the scattering amplitude through the Lüscher method, and resonance properties are inferred.

We suggest it is due to the inclusion of meson-baryon operators that make this coupled-channel $\pi\Sigma - \bar{K}N$ lattice QCD study important to understand the controversial $\Lambda(1405)$. By adding these operators, the full finite-volume energy spectra were obtained, and a comprehensive scattering analysis based on the Lüscher method is possible. Our final results found two poles in the complex energy plane for all parametrizations of the K-matrix. The position of the poles varies slightly for each parametrization, and the best-fit parameter values obtained based on the lowest AIC led to a virtual bound state below the $\pi\Sigma$ threshold ($E_1 = 1392(9)_{\text{st}}(2)_{\text{md}}(16)_a$ MeV) and a resonance just below the $\bar{K}N$ threshold ($E_2 = [1455(13)_{\text{st}}(2)_{\text{md}}(17)_a - i11.5(4.4)_{\text{st}}(4)_{\text{md}}(0.1)_a]$ MeV). These are consistent with the PDG [3], even though we work with slightly unphysical pion and kaon masses.

Future studies exploring the quark-mass-dependence of the pole positions are likely to further improve the understanding of these states. Also, although we work at relatively fine lattice spacing, results at different lattice spacing will be invaluable.

Acknowledgments

We thank our colleagues within the CLS consortium for sharing ensembles. Computations were carried out on Frontera at TACC, and at the (NERSC), a U.S. Department of Energy Office of Science User Facility, located at Lawrence Berkeley National Laboratory, Contract No. DE-AC02-05CH11231 using NERSC, awards NP-ERCAP0005287, NP-RCAP0010836 and NP-ERCAP0015497. Supported in part by: the U.S. National Science Foundation under awards PHY-1913158 and PHY-2209167 (CJM and SK), the Faculty Early Career Development Program (CAREER) under award PHY-2047185 (AN) and by the Graduate Research Fellowship Program under Grant No. DGE-2040435 (JM); the U.S. Department of Energy, Office of Science, Office of Nuclear Physics, under grant contract numbers DE-SC0011090 and DE-SC0021006 (FRL), DE-SC0012704 (ADH), DE-AC02-05CH11231 (AWL) and within the framework of Scientific Discovery through Advanced Computing (SciDAC) award Fundamental Nuclear Physics at the Exascale and Beyond (ADH); the Mauricio and Carlota Botton Fellowship (FRL); and the Heisenberg Programme of the Deutsche Forschungsgemeinschaft project number 454605793 (DM). NumPy [21], matplotlib [22], and the CHROMA software suite [23] were used for analysis, plotting, and correlator evaluation.

References

[1] T. Hyodo, D. Jido, Prog. Part. Nucl. Phys. **67**, 55 (2012), 1104.4474
[2] M. Mai, Few Body Syst. **59**, 61 (2018)
[3] R.L. Workman et al. (Particle Data Group), PTEP **2022**, 083C01 (2022)
[4] R.H. Dalitz, S.F. Tuan, Phys. Rev. Lett. **2**, 425 (1959)

[5] M.H. Alston, L.W. Alvarez, P. Eberhard, M.L. Good, W. Graziano, H.K. Ticho, S.G. Wojcicki, Phys. Rev. Lett. **6**, 698 (1961)
[6] E.A. Veit, B.K. Jennings, R.C. Barrett, A.W. Thomas, Phys. Lett. B **137**, 415 (1984)
[7] B.K. Jennings, Phys. Lett. B **176**, 229 (1986)
[8] P.J. Fink, Jr., G. He, R.H. Landau, J.W. Schnick, Phys. Rev. C **41**, 2720 (1990)
[9] J.A. Oller, U.G. Meissner, Phys. Lett. B **500**, 263 (2001), hep-ph/0011146
[10] D. Jido, J.A. Oller, E. Oset, A. Ramos, U.G. Meissner, Nucl. Phys. A **725**, 181 (2003), nucl-th/0303062
[11] J. Bulava et al. (Baryon Scattering (BaSc)), Phys. Rev. D **109**, 014511 (2024), 2307.13471
[12] J. Bulava et al. (Baryon Scattering (BaSc)), Phys. Rev. Lett. **132**, 051901 (2024), 2307.10413
[13] M. Lüscher, Nucl. Phys. B **354**, 531 (1991)
[14] M. Lüscher, Nucl. Phys. B **364**, 237 (1991)
[15] R.A. Briceno, J.J. Dudek, R.D. Young, Rev. Mod. Phys. **90**, 025001 (2018), 1706.06223
[16] M. Bruno et al., JHEP **02**, 043 (2015), 1411.3982
[17] M. Peardon, J. Bulava, J. Foley, C. Morningstar, J. Dudek, R.G. Edwards, B. Joo, H.W. Lin, D.G. Richards, K.J. Juge (Hadron Spectrum), Phys. Rev. D **80**, 054506 (2009), 0905.2160
[18] C. Morningstar, J. Bulava, J. Foley, K.J. Juge, D. Lenkner, M. Peardon, C.H. Wong, Phys. Rev. D **83**, 114505 (2011), 1104.3870
[19] C. Michael, I. Teasdale, Nucl. Phys. B **215**, 433 (1983)
[20] B. Blossier, M. Della Morte, G. von Hippel, T. Mendes, R. Sommer, JHEP **04**, 094 (2009), 0902.1265
[21] C.R. Harris et al., Nature **585**, 357 (2020), 2006.10256
[22] J.D. Hunter, Comput. Sci. Eng. **9**, 90 (2007)
[23] R.G. Edwards, B. Joo (SciDAC, LHPC, UKQCD), Nucl. Phys. B Proc. Suppl. **140**, 832 (2005), hep-lat/0409003